

Structure of Cs on GaAs(110) as determined by scanning tunneling microscopy

P. N. First, R. A. Dragoset, Joseph A. Stroscio, and R. J. Celotta
National Institute of Standards and Technology, Gaithersburg, Maryland 20899

R. M. Feenstra
IBM T. J. Watson Research Center, Yorktown Heights, New York 10598

(Received 10 February 1989; accepted 31 March 1989)

Submonolayer coverages of Cs adsorbed at room temperature on the GaAs(110) surface are examined with scanning tunneling microscopy. Linear chains, formed by two adjoining rows of Cs atoms, are observed along the $[1\bar{1}0]$ direction for coverages as low as 0.03 monolayer. The one-dimensional Cs chains are observed to be several hundred Å long, and are seen in images of both the occupied and unoccupied electronic states. At higher coverages, approaching 0.15 monolayer, stable linear structures consisting of three neighboring Cs rows have been found.

I. INTRODUCTION

Adsorption of alkali atoms on semiconductor surfaces presents a model system for understanding the evolution of metal-semiconductor interfaces as well as providing an opportunity to probe the physics of low-dimensional systems. Experimentally, the alkali/semiconductor systems are often nonreactive and therefore well defined. Theoretically the alkalis offer simplicity in model calculations because of the singly occupied valence level. The outermost *s*-electron in alkalis is weakly bound, making them very electropositive elements with low work functions in the solid state. A description of the interaction of alkalis with surfaces generally includes a lowering and broadening of the *s*-electron energy level accompanied by partial charge transfer from the alkali to the surface,¹ creating a system of repulsive dipoles for low adatom densities. A partially occupied *s* level has been observed in alkali adsorption on metal surfaces, even for very small coverages.² Dipole repulsion is often the dominant lateral interaction for low coverages and generally gives rise to a disordered or very open structure.³ With increasing coverage, the depolarization caused by adjacent dipoles leads to a lowering of the surface potential and *s* level, causing a decreased charge transfer per atom.

Recently, the question of metallic behavior in alkali/semiconductor systems has received considerable attention.⁴⁻¹⁴ Based on low-energy electron diffraction (LEED) and electron energy loss measurements for K/Si(100), it was concluded that near one-half monolayer (ML) K forms weakly interacting one-dimensional chains on this surface that undergo an insulator-metal transition, due to a decrease in charge transfer, as described above.^{6,7} Dispersion of the energy loss feature was ascribed to one-dimensional plasmon excitations in metallic K chains, a claim which has recently been challenged by theoretical calculations indicating the K overlayer to be ionic up to full coverage.¹²⁻¹⁴

In this paper we report on the subnanometer scale structural and electronic properties of Cs/GaAs(110) observed with scanning tunneling microscopy (STM). Interestingly, it is observed that Cs forms quasi one-dimensional chains on the GaAs(110) surface, even for coverages of as low as 0.03 ML. This is in contrast to the K/Si(100) system, where the

K chains occur as part of a two-dimensional ordered overlayer at $\frac{1}{2}$ monolayer coverage. The one-dimensional character of the atomic Cs chains may provide a model system for testing theories concerning transport and electronic properties of nanometer sized "wires." Here we show the development of the Cs structures as a function of coverage. At low coverages, a two element Cs zig-zag chain is observed. With increased coverage the Cs adsorbates form three element chains which pack together to tile the surface. Voltage dependent imaging shows an increase of state density over the Cs linear structures for both filled and empty energy levels. The sources of this structure and the question of overlayer metallicity are discussed.

II. EXPERIMENTAL

The experiments were performed on two separate systems. The initial data, shown in Fig. 1, are from an experimental system at IBM.¹⁵ The rest of the data are from additional measurements at the National Institute of Standards and Technology (NIST).¹⁶ GaAs samples were cleaved *in situ* under ultrahigh vacuum conditions, base pressure 4×10^{-11} Torr, in order to expose a clean (110) face. The images shown here have the $[1\bar{1}0]$ crystallographic axis oriented at 45° with respect to the $+x$ direction. The orientation of each GaAs wafer ($[001]$ vs $[00\bar{1}]$) was determined using an anisotropic etch after the STM measurements. The wafer orientations were then cross checked with voltage dependent imaging of both the Ga and As atoms,¹⁷ so that the relative positions of the Ga and As atoms could be determined on each sample. After cleaving, Cs was deposited at room temperature using a Cs getter source, with ~ 30 - 100 s deposition times for the images shown here. After deposition, the sample was mounted on the STM for measurement. The NIST STM is similar to an IBM Zurich type microscope employing a glass frame and double spring vibration isolation.¹⁸ A constant tunneling current of 100 pA was used. Both *p*-type and *n*-type samples have been investigated, with similar results for the structures reported here. Coverages quoted were obtained by counting atoms in several images and using the convention that 1 ML corresponds to

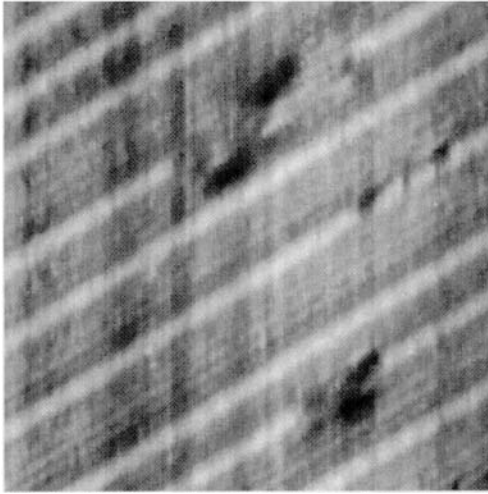


FIG. 1. $155 \times 155 \text{ \AA}$ image of $\sim 0.06 \text{ ML}$ Cs on GaAs(110) (p type, $1 \times 10^{18} \text{ cm}^{-3}$), obtained at -2.7 V sample bias. Cs induced features are observed as the bright linear structures.

a GaAs(110) surface atom density of $8.85 \times 10^{14} \text{ atoms cm}^{-2}$. The images presented here have not been adjusted to account for thermal drift. Images with monatomic steps have their height contrast increased by subtracting a low pass filtered version from the original image.

III. RESULTS

Figure 1 shows the initial measurements of Cs/GaAs(110), obtained with the IBM microscope, in a $155 \times 155 \text{ \AA}$ image at -2.7 V sample bias. Scanning at this voltage, which corresponds to tunneling out of the filled electronic states of GaAs, selectively images the As substrate atoms. Distinct linear chain structures are observed which are continuous over the image, except for some defect regions. The fine rows, between the brighter linear structures, are due to the As sublattice of the substrate. An asymmetry is observed in line profiles perpendicular to the Cs chain structures, with the nearest As row most affected. In Fig. 1, no adsorbate long range order is observed perpendicular to the chain structures. As shown below in higher resolution

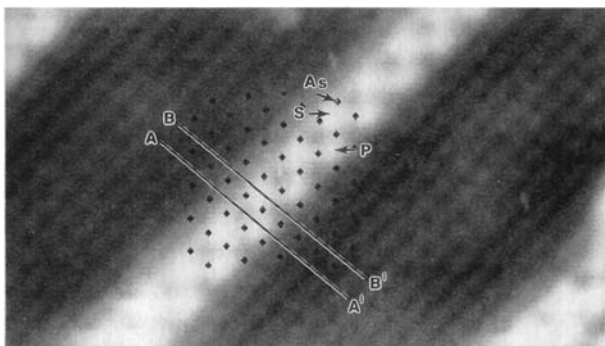


FIG. 2. $160 \times 90 \text{ \AA}$ image of 0.03 ML Cs on GaAs(110) (n type, $2.5 \times 10^{18} \text{ cm}^{-3}$), obtained at -2.4 V sample bias. Primary and secondary Cs maxima are indicated by P and S, respectively. The black diamonds denote the positions of the As atoms, obtained from the As corrugation, for clarity.

images, long range order does exist along the Cs chains.

The higher resolution image in Fig. 2, obtained on the NIST microscope, shows the structure of segments of the Cs chains. In the $160 \times 90 \text{ \AA}$ image of Fig. 2, the Cs chains are seen to consist of a zig-zag structure having two elements, labeled P and S to indicate the primary and secondary Cs maxima. The two Cs maxima are each found to be approximately centered within four surface As atoms, but are distinct from one another due to the anisotropy of the GaAs(110) lattice, which has a two atom basis in the surface unit cell (see Fig. 4). Anisotropy of the GaAs(110) surface manifests itself in the increased STM contour height of the As row immediately to the left of the secondary Cs row, as shown in Fig. 3(a). Note that the corresponding As row, to the right of the primary Cs row, remains largely unaffected. The highlighted As row was found to be reproducible, in particular its relative orientation with respect to the GaAs lattice, for all samples, using different tips and tunneling microscopes.

A geometric model, based on the STM images, is shown in Fig. 4. The relative orientation of the Ga sublattice was determined with anisotropic etching of the samples, as described above. The fact that only the left-most As row is affected arises from the difference between $[001]$ and $[00\bar{1}]$ directions in the GaAs lattice. The two atom basis of the GaAs(110) surface also results in an inequivalence between the primary and secondary Cs atoms, which is discussed further in the next section.

Figure 5 shows an image of Cs/GaAs(110) obtained at positive sample bias, which probes the unoccupied levels. The resolution (and magnification) in this image is substan-

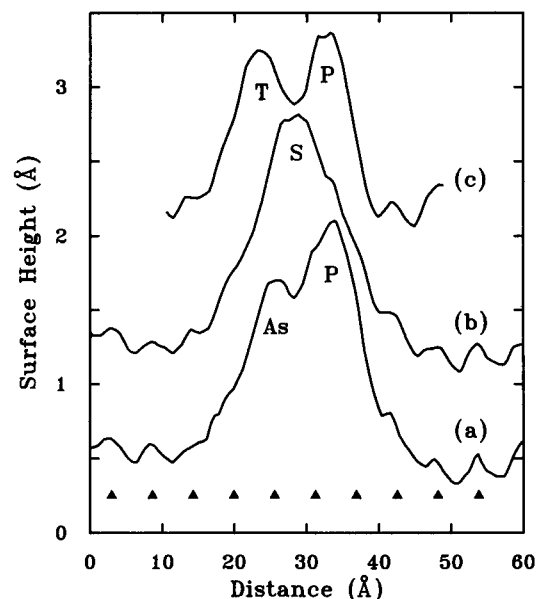


FIG. 3. (a) Profile through the primary Cs maximum along the line A-A' in Fig. 2. The primary maximum and the highlighted As row are labeled P and As, respectively. (b) Profile through the secondary Cs maximum, labeled S, along the line B-B' in Fig. 2. (c) Profile through the primary and tertiary maxima, labeled P and T, along the line A-A' in Fig. 7. The projected As positions in the $(1\bar{1}0)$ plane are indicated by the triangles at the bottom of the figure.

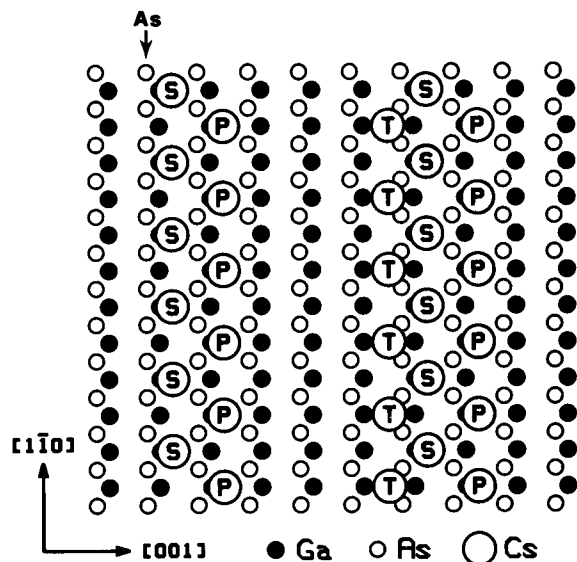


FIG. 4. Schematic diagram showing positions of the Cs induced maxima visible in images of the occupied states (see Figs. 2, 6, and 7). Ga and As are represented by small filled and open circles, respectively, while large circles locate the Cs features, with the enclosed letter identifying primary (P), secondary (S), and tertiary (T) maxima. The structure on the left represents the zig-zag chain of P and S atoms seen in Figs. 2 and 6. The leftmost As row is indicated by an arrow. On the right-hand side is shown the triple chain structure observed in Fig. 7.

tially lower than that of Fig. 2. Difficulties in tunneling to the unoccupied levels are of unknown origin, but may be due to Cs contamination of the tip or perhaps related to a lower barrier height for the cesiated surfaces. This difficulty is not found in other systems such as Fe/GaAs.¹⁹ Figure 5 shows no evidence of the GaAs or Cs corrugations, however we still find distinct row structure due to the Cs. Notice also that these linear structures are not continuous over the monatomic step that appears in the image, but on the lower terrace they are unbroken for ~ 500 Å. It may be possible that structures on the order 1 μm in length could be formed, since cleaved GaAs often yields such step-free terraces.

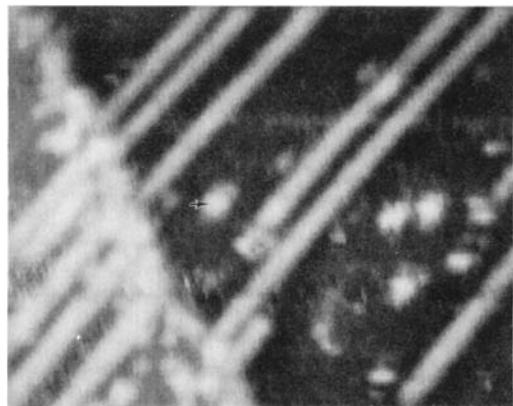


FIG. 5. 600×480 Å image of ~ 0.03 ML Cs on GaAs(110) (*n* type, $2.5 \times 10^{18} \text{ cm}^{-3}$), obtained at +1.5 V sample bias. The upper left region is shown in Fig. 6, imaged at negative sample bias. Note the monatomic step in the center of the image.

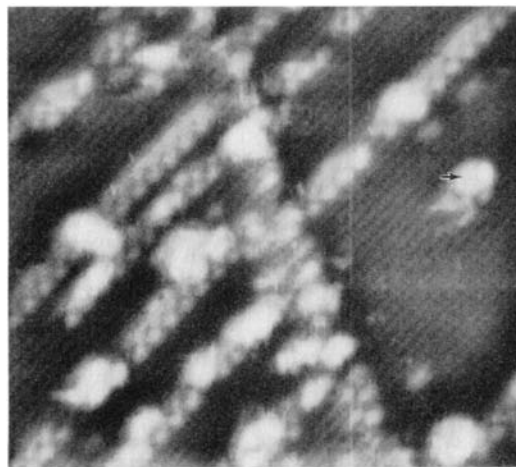


FIG. 6. 300×270 Å image, obtained at -2.4 V sample bias, of a portion of the region shown in Fig. 5. The indicated defect is a common reference point in Figs. 5 and 6.

Figure 6 shows a complementary image of a partial area of Fig. 5, obtained at negative bias. In Figs. 5 and 6 one can see a one to one correspondence between the linear Cs structures in both images. Thus we observe that the Cs chains contribute an increased density of states for both filled and empty electronic levels. At negative bias, higher resolution was obtained and the Cs structures are observed to consist of the zig-zag chains, as depicted in Fig. 4. The appearance of the greater number of defects in Fig. 6, compared to Fig. 5, resulted from successive scanning over the same area at both positive and negative bias.

At higher coverages the formation of three element chains is found, as shown in Fig. 7 for $\Theta \sim 0.13$ ML. The triplet chains are composed of the primary (P) and secondary (S) rows that formed the zig-zag structure, together with a tertiary (T) row, as indicated in Fig. 7. The line profile in Fig. 3(c) shows the tertiary row to be shifted $\sim \frac{1}{4}$ of a lattice spacing toward the primary row, so these Cs maxima are not centered within the four As atoms, as depicted in Fig. 4. This geometry contributes to significant differences in appearance of the three types of rows, as seen in Fig. 7. The primary row appears essentially the same as in previous figures, the secondary maxima are markedly smaller, and the tertiary chain looks much like the primary, except for an apparent delocalization of charge density along the row. In the broken chain segment with line A-A' in Fig. 7, one observes that the primary chain of the first segment smoothly becomes the tertiary chain of the next segment. Close examination of the shorter segment shows a progressive shift of the tertiary chain as it departs from being the primary chain of the previous segment.

Packing of the triple chains is already observed at the Cs coverage of Fig. 7, but the presence of neighboring triplets does not affect the topographic details just described. This suggests weak interaction between triplets, so that the electronic properties of the overlayer may retain quasi one-dimensional characteristics, even near 0.25 ML coverage where an ordered (6×2) phase is observed in LEED.^{20,21}

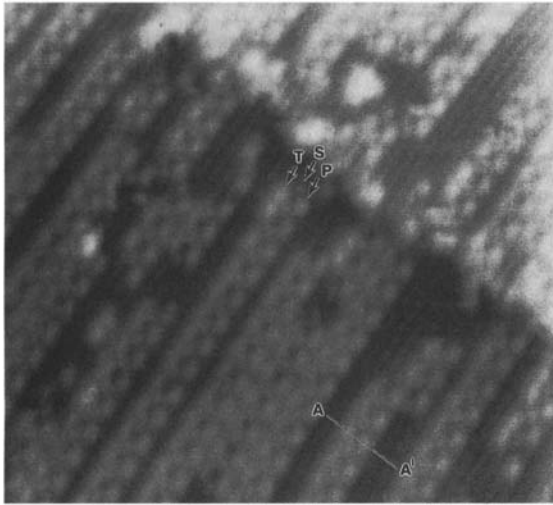


FIG. 7. $300 \times 273 \text{ \AA}$ image of 0.13 ML Cs on GaAs(110) (p type, $5.6 \times 10^{18} \text{ cm}^{-3}$), obtained at -2.6 V sample bias. P, S, and T denote the primary, secondary, and tertiary chain elements, depicted in Fig. 4.

Note that packing the triple chains with a phase shift between neighboring triplets yields a 6×2 structure, perhaps accounting for the 6×2 pattern found in LEED.

IV. DISCUSSION

Since the STM probes electron level densities and not nuclear positions, it is difficult to assess with certainty the true positions of Cs adatoms, however tempting it may be to equate the observed maxima with those positions. Bias dependent imaging demonstrates the hazards of such a naive interpretation.²² Close examination of the images, however, suggests that each maximum is induced by the presence of one Cs adatom, as opposed to the secondary row being due to Cs–Cs or Cs–GaAs interactions, for example. We base this on the observation of discrete maxima in the images, and on the termination of the triple chain structures shown in Fig. 7. Note, for example, that some of the triple chains in Fig. 7 end with a secondary chain maximum and some otherwise identical chains do not. If the secondary row were exclusively due to interaction between the outer two rows or with the substrate, one expects that similar chains should terminate in the same manner. The different end configurations are more easily explained by the presence or absence of one additional Cs atom. From the broken chain segment indicated by the arrow in Fig. 7, one can also see the similarity in the primary and tertiary chain segments, suggesting similar origins for both. This evidence leads us to conclude that each observed maximum in the occupied states corresponds to the presence of one Cs atom, if not to its actual position.

Bonding and electronic properties of the Cs chains are of particular interest in light of the quasi one-dimensional (1-D) geometry of the adsorbed layer. Work function²⁰ and photoemission²³ measurements suggest that Cs donates

much of its valence charge to the substrate upon initial adsorption. If this is the case, one might expect a repulsive interaction between adjacent Cs adatoms, which would evenly disperse them over the surface, as inferred for K on Ni(111), for example.³ On the contrary, formation of the extended chains shown in the figures clearly indicates an attractive interaction between Cs atoms. This does not rule out partial charge transfer to the substrate, but it seems unlikely that the adatoms are fully ionized at any of the coverages shown here. Associating the observed maxima with actual Cs positions gives a Cs–Cs nearest neighbor distance of 6.9 \AA in the zig zag structure, as compared to 5.2 \AA for bulk Cs. Metallic Cs itself is believed to lie close to the Mott metal–insulator transition,²⁴ so it is not yet clear whether the electronic structure of these one-dimensional chains should be that of an insulator or metal, a question that is complicated further by interaction with the substrate. Detailed investigation of the surface electronic structure is being undertaken using current versus voltage measurements. It is worth noting, however, that recent photoemission work²⁵ has concluded that the overlayer is nonmetallic for $< 1 \text{ ML}$ Cs coverage.

The imaging characteristics of the Cs atoms are affected by the electronic structure of the 1-D structures. It is, therefore, worth discussing some of the basic considerations that affect the electronic structure and hence the images. From Fig. 4 one can see that the Cs maxima of the zig-zag structure, labeled P and S, are inequivalent due to the underlying symmetry of the substrate. The asymmetry of the GaAs(110) surface shows up clearly in the Cs induced enhancement of the left-most As row neighboring the secondary Cs row of the zig-zag chains, as described above (see Fig. 3). Considering the geometry in Fig. 4, one sees that the secondary Cs can affect the left As row by bonding to the Ga atoms, which in turn are bonded to the mentioned As atoms. The right-most As row can only be affected indirectly by the primary Cs through back bonds. The inequivalence of the Cs atoms yields a two atom basis in the unit cell of the quasi 1-D chain, and could account for the appearance of two distinct surface core level shifts in photoemission experiments.^{23,26} The two atom basis will create a gap in the electronic energy spectrum of the chain, which, in the absence of any interaction with the substrate, will lie between the filled and empty states, thus forming an insulator. Including charge transfer to the substrate complicates the important question of whether or not the zig-zag chain could be metallic, or perhaps metallize the GaAs surface states, as suggested by recent calculations for K/Si(100).¹² Even if there is partial charge transfer, however, the formation of bonding and antibonding states generally leads to preferential imaging of one basis atom over the other at different tunneling biases, as observed on Si(111) 2×1 and the GaAs(110) surfaces.^{17,27} Images showing different relative intensities of the primary and secondary Cs maxima have been observed; however, detailed voltage dependence of these structures are necessary to reach definite conclusions.

The same considerations outlined above, when applied to the triple chains (with an odd number of electrons in the unit cell), lead to the conclusion that the chains should be metal-

lic in the absence of substrate interaction or a Mott transition. Charge transfer will again profoundly affect this simplistic argument. It is interesting to note the delocalization of charge density along the tertiary row in Fig. 7, which may indicate metallic behavior. A central question in these studies concerns the driving force for forming the linear structures. Preliminary calculations²⁸ suggest that their stability may result from anisotropic dispersion forces associated with the large polarizabilities in the Cs chains. Therefore, it may be that Cs–Cs bonding interactions are indeed the driving force for the formation of these atomic wires, although the substrate clearly plays a crucial role. The final determination of whether these features result from metallic structure must await more detailed measurements.

In conclusion, we have shown that Cs adsorbed on GaAs(110) surfaces at room temperature forms extended linear structures. At low coverages, the Cs atoms form a zigzag chain, which has two inequivalent Cs atoms in the primitive unit cell. At higher coverages a three element chain configuration forms. Differences in appearance among the Cs component elements are attributed to electronic structure resulting from Cs–Cs interactions in the linear structures, but important details of the electronic properties and bonding have yet to be resolved.

ACKNOWLEDGMENTS

We would like to thank M. Krauss and W. Stevens for stimulating discussions, S. Mielczarek and R. Cutkosky for expert technical assistance, and M. Kelley for assistance in image processing. We gratefully acknowledge the partial support of the Office of Naval Research. One of the authors, P. N. F., is a National Research Council postdoctoral associate.

- ¹N. D. Lang, *Phys. Rev. B* **4**, 4 (1971).
- ²B. Woratschek, W. Sesselmann, J. Kupperts, G. Ertl, and H. Haberland, *Phys. Rev. Lett.* **55**, 1232 (1985).
- ³S. Chandavarkar and R. D. Diehl, *Phys. Rev. B* **38**, 12112 (1988).
- ⁴H. Tochihara, *Surf. Sci.* **126**, 523 (1986).
- ⁵H. Ishida, N. Shima, and M. Tsukada, *Surf. Sci.* **158**, 438 (1985).
- ⁶T. Aruga, H. Tochihara, and Y. Murata, *Phys. Rev. Lett.* **53**, 372 (1984).
- ⁷M. Tsukada, H. Ishida, and N. Shima, *Phys. Rev. Lett.* **53**, 376 (1984).
- ⁸R. V. Kasowski and M.-H. Tsai, *Phys. Rev. Lett.* **60**, 546 (1988).
- ⁹H. Tochihara, M. Kubota, M. Miyao, and Y. Murata, *Surf. Sci.* **158**, 497 (1985).
- ¹⁰H. Tochihara, M. Kubota, T. Aruga, M. Miyao, and Y. Murata, *Jpn. J. Appl. Phys.* **23**, L271 (1984).
- ¹¹H. Tochihara and Y. Murata, *J. Phys. Soc. Jpn.* **51**, 2920 (1982).
- ¹²S. Ciraci and I. P. Batra, *Phys. Rev. Lett.* **56**, 877 (1986).
- ¹³I. P. Batra and P. S. Bagus, *J. Vac. Sci. Technol.* **6**, 600 (1988).
- ¹⁴S. Ciraci and I. P. Batra, *Phys. Rev. Lett.* **60**, 547 (1988).
- ¹⁵The IBM microscope used here is a second generation hybrid design consisting of single spring suspension with viton separated stacked plates.
- ¹⁶R. A. Dragoset, R. D. Young, H. P. Layer, S. R. Mielczarek, E. C. Teague, and R. J. Celotta, *Opt. Lett.* **11**, 560 (1987).
- ¹⁷R. M. Feenstra, J. A. Stroscio, J. Tersoff, and A. P. Fein, *Phys. Rev. Lett.* **58**, 1192 (1987).
- ¹⁸G. Binnig and H. Rohrer, *Sci. Am.* **253**, 50 (1985).
- ¹⁹P. N. First, J. A. Stroscio, R. A. Dragoset, D. T. Pierce, and R. J. Celotta (to be published).
- ²⁰J. Derrien and F. Arnaud D'Avitaya, *Surf. Sci.* **65**, 668 (1977).
- ²¹A. J. van Bommel and J. E. Crombeen, *Surf. Sci.* **45**, 308 (1974).
- ²²J. A. Stroscio, R. M. Feenstra, and A. P. Fein, *J. Vac. Sci. Technol. A* **5**, 838 (1987).
- ²³M. Prietsch, M. Domke, C. Laubschat, T. Mandel, C. Xue, and G. Kaindl, *Z. Phys. B* **74**, 21 (1989).
- ²⁴A. Ferraz, N. H. March, and F. Flores, *J. Phys. Chem. Solids* **45**, 627 (1984).
- ²⁵T. M. Wong, D. Heskett, N. J. DiNardo, and E. W. Plummer, *Surf. Sci. Lett.* **208**, L1 (1989). Note the different definition of 1 monolayer.
- ²⁶T. Kendelewicz, P. Soukiassian, M. H. Bakshi, Z. Hurych, I. Lindau, and W. E. Spicer, *Phys. Rev. B* **38**, 7568 (1988).
- ²⁷J. A. Stroscio, R. M. Feenstra, and A. P. Fein, *Phys. Rev. Lett.* **57**, 2579 (1986).
- ²⁸M. Krauss and W. J. Stevens (private communication).